Radiation Physics Note 92

Vasek Vylet

October 16, 1991

ESTIMATED SENSITIVITY OF THE "MUON GUN" TO NEUTRONS

Introduction

The "Muon Gun" is an an assembly of two plastic scintillators mounted on their photomultipliers, aligned within an aluminum tube. With the two scintillators kept apart at a sufficient distance, the device can be used as a "telescope" to determine the direction of incoming muons by counting the coincidences in both detectors. Unfortunately, the plastic scintillator (Pilot B) is also sensitive to neutrons, due to its high content of hydrogen. The purpose of this note is to provide a simple estimate of this neutron sensitivity. In the first step a calculation of the neutron efficiency was performed, taking a number of simplifying assumptions. The second step consisted of verifying calculated results experimentally, using Am-Be and ^{60}Co sources.

Calculations

Each of the two scintillators is a circular disk 0.635 cm (1/4") thick with a diameter of 2.13 cm. These dimensions are smaller than the mean free path of neutrons with energies greater than a few hundred keV. In first approximation we can assume that the scintillator response to these neutrons will be determined by the number of the first collisions with hydrogen. Under this assumption the probability that a neutron impinging on the scintillator will cause an interaction is

$$\varepsilon_H = \frac{\Sigma_H}{\Sigma_{tot}} (1 - e^{-L.\Sigma_{tot}})$$

where L is the mean chord, Σ_{tot} is the total macroscopic cross section and Σ_H is the hydrogen contribution to Σ_{tot}†. Macroscopic cross sections for Pilot F were computed using microscopic cross sections for hydrogen and carbon from the MATXS6 library for 80 energy groups between thermal and 20 MeV. The results are presented in Appendix A.

---

† $\Sigma_{tot} = n_C\sigma_C + n_H\sigma_H$ and $\Sigma_H = n_H\sigma_H$, where n_C and n_H are the densities of atoms and σ_C and σ_H are the microscopic cross sections for carbon and hydrogen, respectively.

Although the contribution of the recoiled carbon ion to the scintillator signal can in first approximation be neglected, neutrons recoiled from these carbon nuclei can still undergo one or more collisions with hydrogen, if the dimensions of the scintillator are not extremely small in comparison with the neutron mean free path. Elwyn et al.[1] devised a method to calculate this contribution for cylindrical scintillators, assuming that the recoiled neutron sees a spherical scintillator of the same volume. This approach enables an analytical solution of the problem, leading to the following results :

$$\varepsilon_{tot} = \frac{\varepsilon_H}{1 - (1 - \frac{\Sigma_H}{\Sigma_{tot}})p_2} \quad ,$$

where ε_{tot} is the corrected efficiency and p_2 is the probability that a neutron will interact with hydrogen after scattering from carbon. It is given as

$$p_2 = 1 - \frac{3}{2x}\left(1 - \frac{2}{x^2}\right) - \frac{3}{x^2}e^{-x}\left(1 + \frac{1}{x}\right)$$

where $x = 2R\Sigma_{tot}$, R being the radius of the hypothetical sphere.

In the following, neutron efficiencies ε_{tot} and ε_H were calculated with and without the above correction, respectively. This correction is best suited to orthocylindrical volumes, i.e. with the length of the cylinder comparable to its diameter. For a "flat" cylinder as in our case the distribution of possible path lengths through the scintillator from the recoil point will be different. It will favor shorter lengths and this procedure would therefore overestimate the amount of correction needed. For this reason, ε_{tot} should be considered in our case as an upper limit of the estimate.

Three different irradiation geometries were considered in the calculations of neutron efficiency :

A. "Face" irradiation, i.e. a parallel beam perpendicular to the circular surface, along the main axis of the cylinder. The mean chord here is the scintillator thickness - 0.635 cm.

B. "Side" irradiation, i.e. a parallel beam perpendicular to the main cylinder axis. The mean chord can be then calculated as indicated below :

$$\frac{L}{2} = \frac{\int_0^R \sqrt{R^2-x^2}\,dx}{\int_0^R R.dx}$$

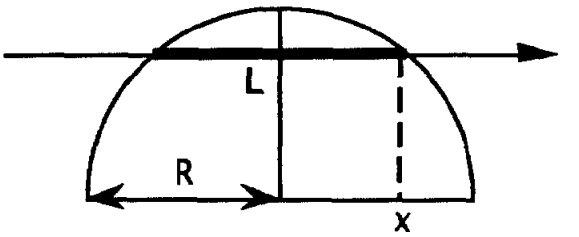

It follows from the above formula that $L = \frac{\pi}{2} R$, which is in our case 1.67 cm.

C. Isotropic irradiation - in this case L = 4V/S, where V and S are the volume and the surface of the scintillator, respectively. For this geometry L = 0.796 cm.

Calculated efficiencies for 3 different energies are presented in Table 1. Note that efficiency scales approximately as the mean chord*. A more detailed calculation for isotropic geometry only is presented in the Appendix B for energies between 0.1 and 20 MeV. For the sake of comparison, Appendix B also includes ε calculated for a larger scintillator "paddle" used in the MERL (8"x8"x1/4"). Concerning the paddle, the ε_{tot} "isotropic" value of 19% at 4.2 MeV is in reasonably good agreement with 7.4% found previously by Alex Elwyn[2] for the "face" geometry, taking into account the scaling noted above with the mean chord. (The ratio of the mean chords is 2.9).

Energy	Geometry	L	ε_H	ε_{tot}
4.2 MeV	face	0.635	0.0609	0.0641
	side	1.670	0.1456	0.1533
	isotropic	0.796	0.0752	0.0791
1.1 MeV	face	0.635	0.1252	0.1333
	side	1.670	0.2801	0.2983
	isotropic	0.796	0.1529	0.1628
0.1 MeV	face	0.635	0.3376	0.3708
	side	1.670	0.6013	0.6603
	isotropic	0.796	0.3964	0.4353

Table 1 : Calculated efficiencies for a Ø 2.13 x 0.635 cm Pilot F scintillator

Calibrations using neutron and gamma sources

An Am-Be neutron source (241Be-6.7-1, emission = 6.80E+6 s^{-1}) was used to check the scintillator sensitivity in "face" and "side" irradiation geometries. Only the "front" scintillator was used here, since it is possible to adjust its position in front of a small hole in the middle of the aluminum tube housing.

* This follows from $1-e^{-x} \approx x$ for sufficiently large x

This hole was a convenient reference point in setting up the irradiation geometry and measuring the distance to the source. Results of this irradiation are summarized in Table 2 below.

Geometry	Time [s]	Distance [cm]	N
background	120	-	393
face	300	66	8662
side	300	30	56282
side	240	23	76764

Table 2 : Irradiation with an Am-Be source

Irradiations were performed in the source projector facility, with the source mounted on a stand and the Muon Gun positioned at the edge of an aluminum table ~100 cm above the ground. In the "face" geometry the photomultiplier was between the source and the scintillator. No attempt was made to correct for the presence of the surrounding material (housing, PM) or to allow for the contribution of room scattering. Since the resolving time[3] is only 250 ns , no correction was necessary at the above counting rates.

The Am-Be source was covered with a 1/16" thick lead cap to eliminate its 59.5 keV gamma radiation. However, high energy gamma rays from the ^{12}C de-excitation after an (α,n) reaction on beryllium (~4.4 MeV) will still be present. In the first step the contribution from this gamma component was ignored. Sensitivities derived from the Am-Be irradiation under these conditions are presented in Table 3 and compared with the calculated values for 4.2 MeV, which is close to the mean neutron energy of the Am-Be spectrum.

Geometry	ε [%] (Am-Be)	ε_H, ε_{tot} [%] (calculated)
face	5.7	6.1-6.4
side	22.4	14.6-15.3
side	18.0	14.6-15.3

Table 3 : Measured neutron sensitivities, no correction for gammas.

In order establish the sensitivity of the Muon Gun to gamma radiation, an irradiation with a ^{60}Co (60-4.3-2) source was performed. In "face" geometry the sensitivity was found to be 164,202. $mrad^{-1}$; for the "side" geometry it was 242,986. $mrad^{-1}$. One can assume that these sensitivities would be lower for higher energy gamma radiation by a factor of

$$\frac{1 - e^{-\mu_\rho(4.4\ \mathrm{MeV}).L.\rho}}{1 - e^{-\mu_\rho(1\ \mathrm{MeV}).L.\rho}} \quad ,$$

which yields 78,817. $mrad^{-1}$ and 111,774. $mrad^{-1}$ for face and side geometries, respectively, using $\mu_{\rho(1\ \mathrm{MeV})} = 0.069\ cm^2/g$ and $\mu_{\rho(4.4\ \mathrm{MeV})} = 0.031\ cm^2/g$ for polystyrene[4].

The gamma dose rate from the Am-Be (241Be-6.7-1) source was estimated by scaling down the results of a measurement[5] performed by F. Krueger for a different source of the same type (241Be-7.2-1). Using a large Al-Ar ionization chamber (calibrated to ^{60}Co), a value of 0.654 mrad/h at 1 m was found for the latter source. Assuming that the ratio of neutron emission and gamma dose rate is approximately the same for the two Am-Be sources in question, the gamma dose rate at 1 m from the 241Be-6.7-1 source was estimated to 0.222 mrad/h. Using this value and the above gamma sensitivities, the gamma contribution to the total detector response was established to be about 39% for both side and face geometries. This procedure implicitly assumes that the response of the Al-Ar chamber (current per dose) is the same at 1 and 4.4 MeV. Table 4 presents the neutron sensitivities, when the gamma contribution to the signal is subtracted, compared again to the calculated values.

Geometry	ε [%] (Am-Be)	ε_H, ε_{tot} [%] (calculated)
face	3.5	6.1-6.4
side	13.5	14.6-15.3
side	11.0	14.6-15.3

Table 4 : Measured neutron sensitivities, gamma contribution corrected

Conclusions

The results in tables 3 and 4 are the product of rather crude measurements coupled with many simplifying assumptions and approximations, and this leads speculation about the observed discrepancies. Higher measured than calculated values in Table 3 seem to indicate an uncorrected gamma contribution. Lower measured values in Table 4 might result either from an exaggerated gamma correction, or a loss of detection efficiency not accounted for in the calculations.

In an unknown neutron field, isotropic irradiation geometry should be assumed, for which we do not have a calibration measurement. The calculated sensitivities presented in Table 1 and Appendix B might offer a reasonable estimate.

Thanks to Alex Elwyn for helpful discussions, suggestions and editorial comments, Fred Krueger and John Larson for providing useful information and data about the detectors and Anil Kumar (UCLA) for providing the microscopic cross sections.

References

(1) A. Elwyn et al. : "Reaction $C^{12}(d,n)N^{13}$", The Physical. Review, Vol. 116, No. 6, pp. 1490-1498, December 15, 1959
(2) A. Elwyn - private communication
(3) J. Larson, private communication
(4) The Health Physics and Radiological Health Handbook, Nucleon Lectern Associates, 1984
(5) F. Krueger : Radiation Physics note 86 and private communication.

APPENDIX A : Macroscopic cross-sections for Pilot F

[$\rho = 1.03$ g/cm^3 H/C ratio = 1.103 neglecting other elements]

Group	E [MeV] up bound	E [MeV] log mean	σ_H [barn]	σ_C [barn]	Σ_{tot} [cm^{-1}]	λ_{tot} [cm]	Σ_H [cm^{-1}]	λ_H [cm]
1	2.00E+1	1.84E+1	0.57	1.22	0.0873	11.46	0.0295	33.90
2	1.69E+1	1.59E+1	0.66	1.23	0.0929	10.76	0.0347	28.84
3	1.49E+1	1.42E+1	0.72	1.12	0.0905	11.05	0.0375	26.67
4	1.35E+1	1.27E+1	0.78	1.16	0.0956	10.46	0.0407	24.55
5	1.19E+1	1.09E+1	0.93	1.10	0.1004	9.96	0.0484	20.68
6	1.00E+1	8.83E+0	1.11	1.21	0.1152	8.68	0.0580	17.25
7	7.79E+0	6.88E+0	1.36	1.12	0.1240	8.06	0.0710	14.08
8	6.07E+0	5.35E+0	1.64	1.12	0.1387	7.21	0.0856	11.68
9	4.72E+0	4.17E+0	1.95	1.87	0.1903	5.25	0.1018	9.82
10	3.68E+0	3.25E+0	2.29	2.23	0.2251	4.44	0.1196	8.36
11	2.87E+0	2.53E+0	2.66	1.73	0.2208	4.53	0.1389	7.20
12	2.23E+0	1.97E+0	3.08	1.82	0.2470	4.05	0.1608	6.22
13	1.74E+0	1.53E+0	3.54	2.01	0.2800	3.57	0.1848	5.41
14	1.35E+0	1.27E+0	3.92	2.26	0.3117	3.21	0.2047	4.89
15	1.19E+0	1.12E+0	4.19	2.43	0.3338	3.00	0.2188	4.57
16	1.05E+0	9.88E-1	4.47	2.59	0.3560	2.81	0.2334	4.28
17	9.30E-1	8.74E-1	4.78	2.76	0.3802	2.63	0.2496	4.01
18	8.21E-1	7.71E-1	5.10	2.92	0.4045	2.47	0.2663	3.76
19	7.24E-1	6.80E-1	5.45	3.07	0.4299	2.33	0.2846	3.51
20	6.39E-1	6.00E-1	5.83	3.21	0.4564	2.19	0.3044	3.29
21	5.64E-1	5.30E-1	6.22	3.35	0.4834	2.07	0.3248	3.08
22	4.98E-1	4.68E-1	6.64	3.47	0.5110	1.96	0.3467	2.88
23	4.39E-1	4.13E-1	7.08	3.59	0.5396	1.85	0.3697	2.71
24	3.88E-1	3.42E-1	7.81	3.75	0.5853	1.71	0.4078	2.45
25	3.02E-1	2.66E-1	8.83	3.94	0.6476	1.54	0.4611	2.17
26	2.35E-1	2.07E-1	9.93	4.10	0.7126	1.40	0.5185	1.93
27	1.83E-1	1.62E-1	11.10	4.23	0.7798	1.28	0.5796	1.73
28	1.43E-1	1.26E-1	12.20	4.33	0.8420	1.19	0.6370	1.57
29	1.11E-1	9.80E-2	13.40	4.41	0.9084	1.10	0.6997	1.43
30	8.65E-2	7.64E-2	14.50	4.48	0.9692	1.03	0.7571	1.32
31	6.74E-2	5.95E-2	15.60	4.54	1.0295	0.97	0.8146	1.23
32	5.25E-2	4.63E-2	16.50	4.58	1.0784	0.93	0.8615	1.16
33	4.09E-2	3.61E-2	17.30	4.61	1.1216	0.89	0.9033	1.11
34	3.18E-2	2.99E-2	17.90	4.63	1.1538	0.87	0.9346	1.07
35	2.81E-2	2.71E-2	18.20	4.64	1.1700	0.85	0.9503	1.05
36	2.61E-2	2.54E-2	18.30	4.65	1.1757	0.85	0.9555	1.05
37	2.48E-2	2.33E-2	18.60	4.65	1.1913	0.84	0.9712	1.03
38	2.19E-2	2.06E-2	18.80	4.66	1.2022	0.83	0.9816	1.02
39	1.93E-2	1.81E-2	19.10	4.67	1.2184	0.82	0.9973	1.00
40	1.70E-2	1.60E-2	19.30	4.68	1.2293	0.81	1.0077	0.99
41	1.50E-2	1.41E-2	19.50	4.69	1.2402	0.81	1.0182	0.98
42	1.33E-2	1.25E-2	19.70	4.69	1.2507	0.80	1.0286	0.97
43	1.17E-2	1.10E-2	19.90	4.70	1.2616	0.79	1.0391	0.96
44	1.03E-2	9.69E-3	20.10	4.70	1.2720	0.79	1.0495	0.95
45	9.12E-3	8.57E-3	20.20	4.70	1.2772	0.78	1.0547	0.95
46	8.05E-3	7.56E-3	20.30	4.71	1.2829	0.78	1.0600	0.94
47	7.10E-3	6.67E-3	20.40	4.71	1.2882	0.78	1.0652	0.94
48	6.27E-3	5.89E-3	20.50	4.71	1.2934	0.77	1.0704	0.93
49	5.53E-3	5.19E-3	20.60	4.72	1.2991	0.77	1.0756	0.93

Group	E [MeV] up bound	E [MeV] log mean	σ_H [barn]	σ_C [barn]	Σ_{tot} [cm^{-1}]	λ_{tot} [cm]	Σ_H [cm^{-1}]	λ_H [cm]
50	4.88E-3	4.59E-3	20.70	4.72	1.3043	0.77	1.0809	0.93
51	4.31E-3	4.05E-3	20.80	4.72	1.3095	0.76	1.0861	0.92
52	3.80E-3	3.57E-3	20.80	4.72	1.3095	0.76	1.0861	0.92
53	3.35E-3	3.15E-3	20.90	4.72	1.3147	0.76	1.0913	0.92
54	2.96E-3	2.78E-3	20.90	4.73	1.3152	0.76	1.0913	0.92
55	2.61E-3	2.46E-3	21.00	4.73	1.3204	0.76	1.0965	0.91
56	2.31E-3	2.17E-3	21.00	4.73	1.3204	0.76	1.0965	0.91
57	2.03E-3	1.91E-3	21.10	4.73	1.3256	0.75	1.1017	0.91
58	1.80E-3	1.69E-3	21.10	4.73	1.3256	0.75	1.1017	0.91
59	1.58E-3	1.49E-3	21.10	4.73	1.3256	0.75	1.1017	0.91
60	1.40E-3	1.31E-3	21.10	4.73	1.3256	0.75	1.1017	0.91
61	1.23E-3	1.16E-3	21.20	4.73	1.3309	0.75	1.1070	0.90
62	1.09E-3	1.02E-3	21.20	4.73	1.3309	0.75	1.1070	0.90
63	9.61E-4	8.48E-4	21.20	4.74	1.3313	0.75	1.1070	0.90
64	7.49E-4	6.61E-4	21.20	4.74	1.3313	0.75	1.1070	0.90
65	5.83E-4	5.14E-4	21.30	4.74	1.3366	0.75	1.1122	0.90
66	4.54E-4	4.01E-4	21.30	4.74	1.3366	0.75	1.1122	0.90
67	3.54E-4	3.12E-4	21.30	4.74	1.3366	0.75	1.1122	0.90
68	2.75E-4	2.14E-4	21.30	4.74	1.3366	0.75	1.1122	0.90
69	1.67E-4	1.30E-4	21.30	4.74	1.3366	0.75	1.1122	0.90
70	1.01E-4	7.87E-5	21.30	4.74	1.3366	0.75	1.1122	0.90
71	6.14E-5	4.79E-5	21.30	4.74	1.3366	0.75	1.1122	0.90
72	3.73E-5	2.90E-5	21.30	4.74	1.3366	0.75	1.1122	0.90
73	2.26E-5	1.76E-5	21.30	4.74	1.3366	0.75	1.1122	0.90
74	1.37E-5	1.07E-5	21.40	4.74	1.3418	0.75	1.1174	0.89
75	8.32E-6	6.48E-6	21.40	4.74	1.3418	0.75	1.1174	0.89
76	5.04E-6	3.93E-6	21.40	4.74	1.3418	0.75	1.1174	0.89
77	3.06E-6	1.86E-6	21.50	4.74	1.3470	0.74	1.1226	0.89
78	1.13E-6	6.84E-7	21.80	4.75	1.3631	0.73	1.1383	0.88
79	4.14E-7	2.51E-7	22.60	4.76	1.4054	0.71	1.1801	0.85
80	1.52E-7	4.59E-9	27.10	4.86	1.6451	0.61	1.4150	0.71
l.b.	1.4E-10							

APPENDIX B: Neutron efficiency for scintillators of different size

E [MeV] (log interval mean)	ε_H paddle L = 1.8208 cm	ε_H gun L = 0.7956 cm	ε_{tot} paddle L = 1.8208 cm	ε_{tot} gun L = 0.7956 cm
18.385	0.0497	0.0227	0.0580	0.0235
15.869	0.0581	0.0266	0.0678	0.0275
14.183	0.0629	0.0288	0.0724	0.0297
12.675	0.0681	0.0312	0.0787	0.0322
10.909	0.0805	0.0370	0.0921	0.0381
8.826	0.0952	0.0441	0.1101	0.0456
6.876	0.1157	0.0538	0.1320	0.0555
5.353	0.1378	0.0645	0.1566	0.0665
4.168	0.1567	0.0752	0.1919	0.0791
3.250	0.1786	0.0871	0.2251	0.0925
2.530	0.2082	0.1013	0.2483	0.1062
1.970	0.2358	0.1162	0.2817	0.1219
1.533	0.2637	0.1318	0.3179	0.1390
1.267	0.2844	0.1442	0.3481	0.1530
1.118	0.2985	0.1529	0.3688	0.1628
0.988	0.3127	0.1617	0.3893	0.1729
0.874	0.3279	0.1713	0.4113	0.1839
0.771	0.3431	0.1812	0.4330	0.1951
0.680	0.3593	0.1917	0.4555	0.2071
0.600	0.3765	0.2031	0.4785	0.2200
0.530	0.3932	0.2145	0.5011	0.2330
0.468	0.4109	0.2267	0.5238	0.2467
0.413	0.4286	0.2391	0.5464	0.2609
0.342	0.4567	0.2594	0.5809	0.2836
0.266	0.4930	0.2867	0.6240	0.3142
0.207	0.5288	0.3149	0.6647	0.3457
0.162	0.5636	0.3436	0.7024	0.3775
0.126	0.5932	0.3694	0.7334	0.4059
0.098	0.6229	0.3963	0.7631	0.4353